C2GT

Intercepting CERN neutrinos to Gran Sasso in the Gulf of Taranto to measure θ_{13}

Presented by F. Dydak (CERN)

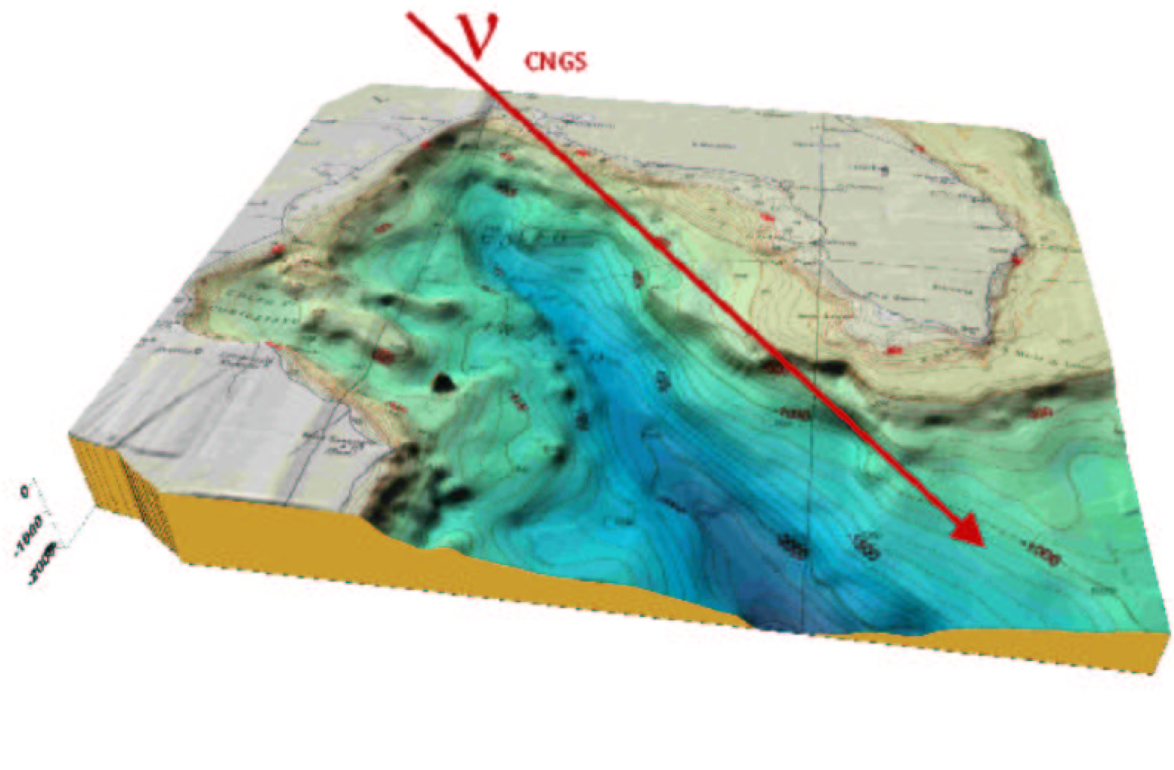

Figure 1: The deep-sea trench in the Gulf of Taranto

Measuring $\sin^2\theta_{13}$

Planetary neutrino oscillations are well described by

$$\begin{aligned} P(\nu_\mu \to \nu_\mathrm{e}) &\cong \sin^2\theta_{23}\,\sin^2 2\theta_{13}\,\sin^2\left(\frac{1.27\Delta m^2_{23}\,L}{E_\nu}\right) , \\ P(\nu_\mathrm{e} \to \nu_\tau) &\cong \cos^2\theta_{23}\,\sin^2 2\theta_{13}\,\sin^2\left(\frac{1.27\Delta m^2_{23}\,L}{E_\nu}\right) , \\ P(\nu_\mu \to \nu_\tau) &\cong \cos^4\theta_{13}\,\sin^2 2\theta_{23}\,\sin^2\left(\frac{1.27\Delta m^2_{23}\,L}{E_\nu}\right) . \end{aligned}$$

For measuring $\sin^2\theta_{13}$: select $\nu_\mu \to \nu_\mathrm{e}$

For the transition $\nu_\mu \leftrightarrow \nu_\mathrm{e}$ at the maximum of the oscillation, the oscillation probability is:

$$P(\nu_\mathrm{e} \to \nu_\mu) \cong 2\sin^2\theta_{13} \ .$$

Needs a monoenergetic low-energy ν_μ beam

- to permit a detector location at the maximal oscillation amplitude within a realistic distance
- to permit the suppression of NC-induced background

Off-axis geometry

The longitudinal and transverse momenta of the ν_μ in the laboratory system are

$$\begin{aligned} p_{\rm L} &= \gamma(p^* \cos\Theta^* + \beta p^*) \\ p_{\rm T} &= p^* \sin\Theta^* \,, \end{aligned}$$

$p^* = 0.03$ GeV$/c$ = neutrino momentum
Θ^* = polar angle of neutrino emission w.r.t. the π direction of flight. For $\Theta^* = 90°$:

$$\Theta = \frac{1}{\gamma} \,.$$

Neutrino flux:

$$\Phi_\nu(R) = \frac{\frac{\gamma^2}{\pi L^2}}{\left(1 + (\gamma \frac{R}{L})^2\right)^2} \,,$$

All-important feature:

$$\frac{\partial E_\nu}{\partial \gamma} = 0 \,.$$

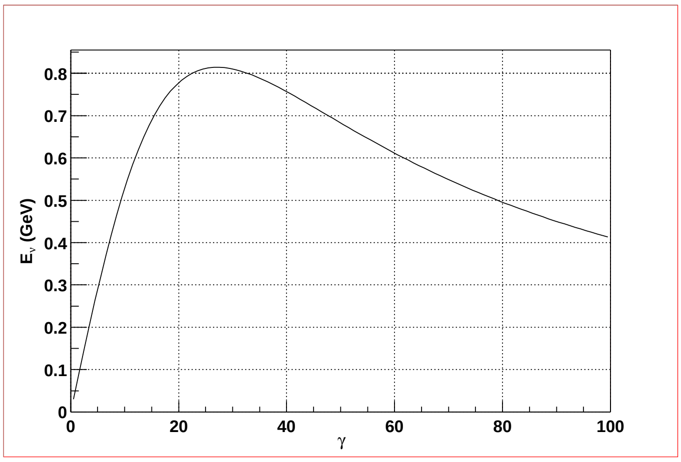

Figure 2: Neutrino energy from π decay as a function of γ_π at an off-axis angle $\theta = 1/27.1$.

Off-axis neutrinos in the Gulf of Taranto

Table 1: Parameters of neutrino beam and detector for a distance of 1200 km from CERN.

Distance L from CERN [km]	1200
Geodesic longitude	017° 54’ E
Geodesic latitude	39° 47’ N
Radial distance R from CNGS beam axis [km]	44
γ of parent pion	27.1
Parent-pion momentum [GeV/c]	3.8
Neutrino flux per decaying pion [cm^{-2}]	4.1×10^{-15}
Neutrino energy from pion decay [GeV]	0.81
Neutrino energy from Kaon decay [GeV]	3.4

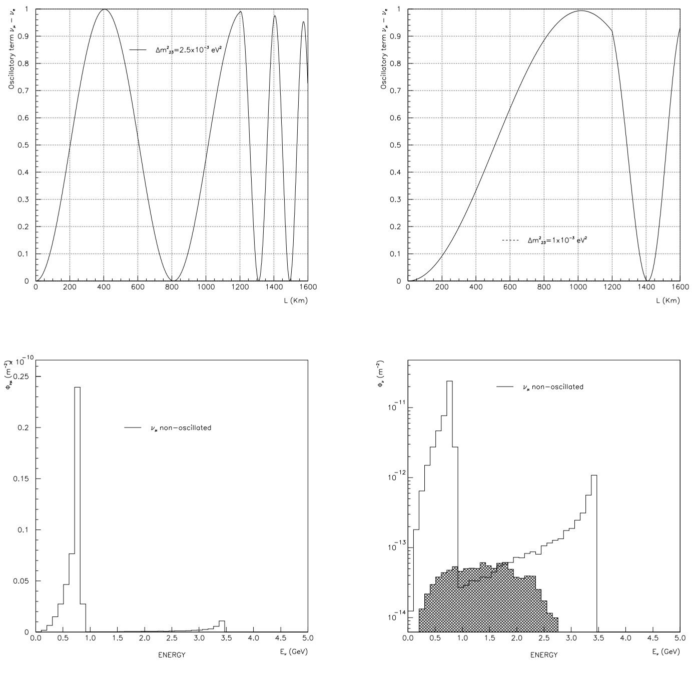

Figure 3: Oscillation pattern (top), neutrino flux bottom)

Schematics of the deep-sea detector

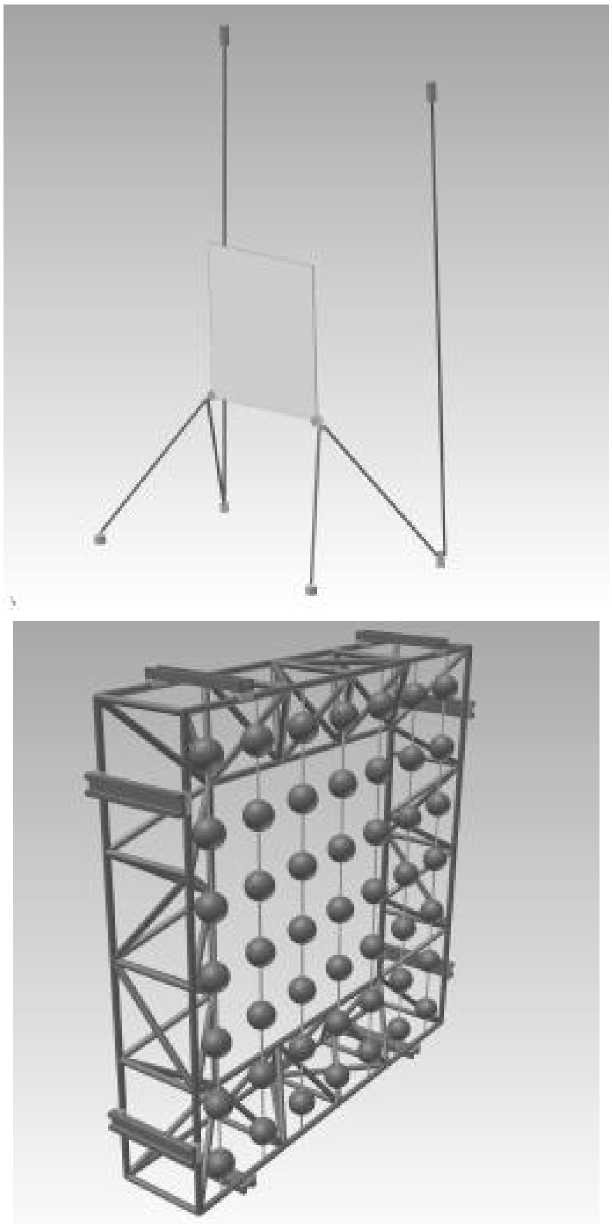

Figure 4: Detector plane (top); 10 m $\times$ 10 m Mechanical Module (bottom)

Optical module

- efficient light detection in the wavelength range 300 – 550 nm;
- maximal surface and angular acceptance;
- sensitivity to a single photoelectron;
- timing resolution $\leq$ 2 ns;
- dark count probability $\leq$ 0.1 photoelectron within a time window of 100 ns;
- operation in sea water at a depth of $\sim$ 1000 m.

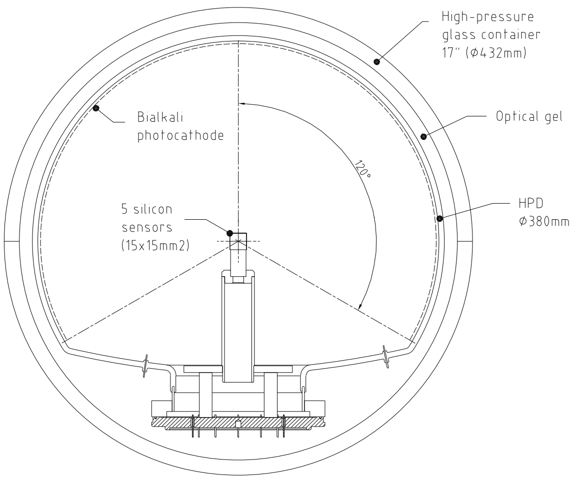

Figure 5: Schematic view of the Optical Module (left), 3D schematic of the Optical Module (right).

Pion production in target

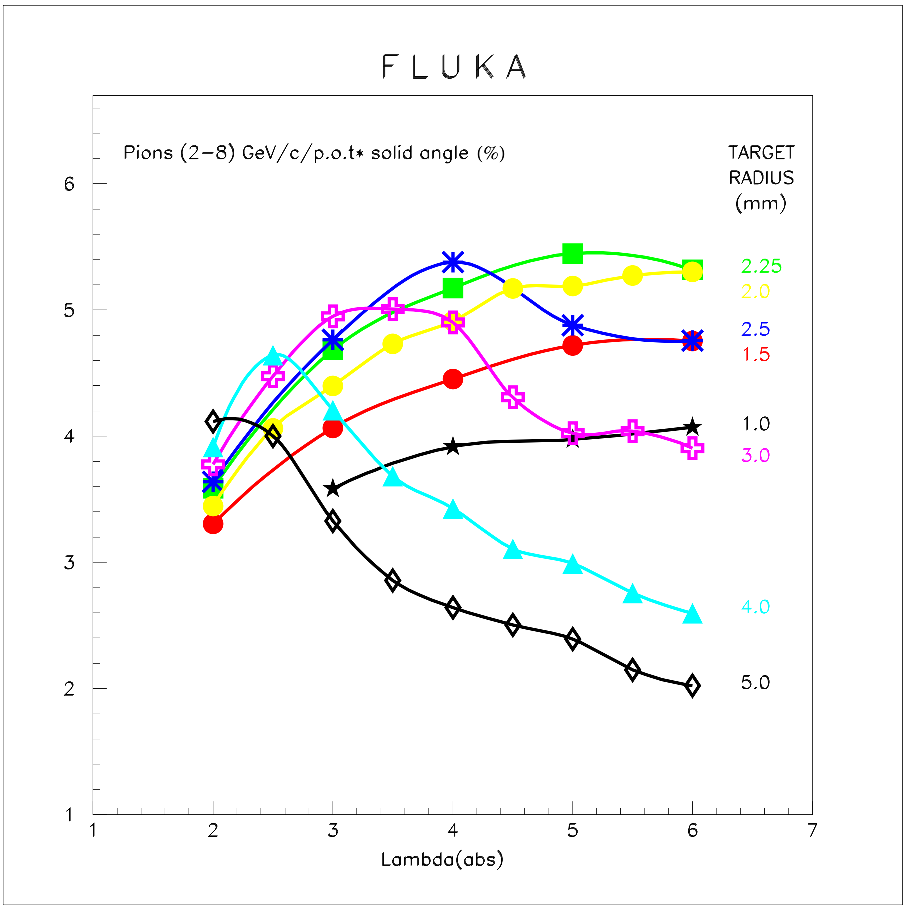

Figure 6: Yield of $\pi^{\pm}$ from rotationally symmetric graphite targets with different absorption lengths and radii.

3.3 π^+ per proton with momenta between 2 and 8 GeV/c and polar angle $\leq$ 200 mrad are used to estimate the neutrino flux.

With 'ideal' horn focussing, out of the initial 3.3 π^+ per proton, 1.5 can be bent parallel to the horn axis.

Photon emission by electrons and muons of 800 MeV

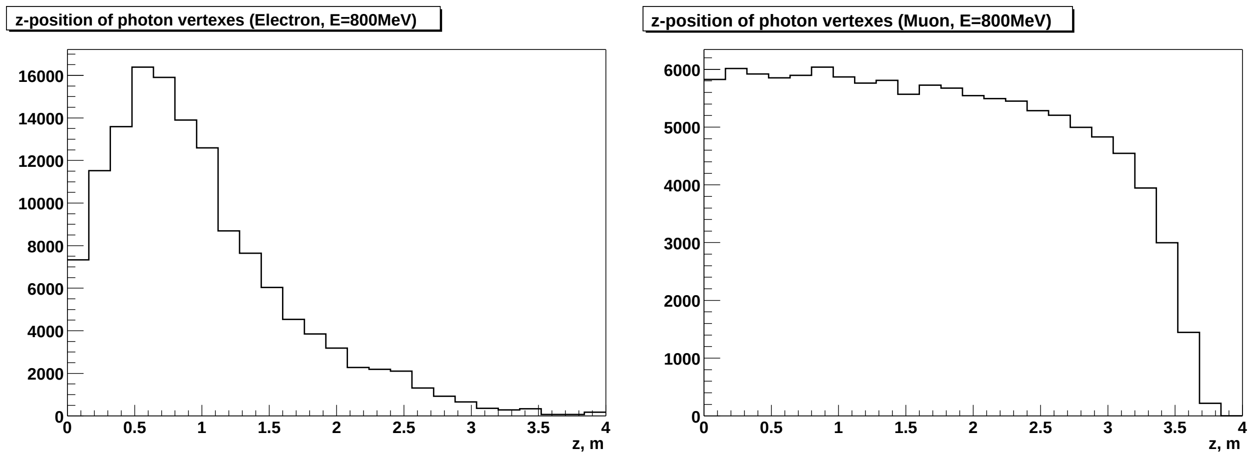

Figure 7: Distance of emission of Cherenkov photons from the vertex, for 800 MeV electrons (top) and muons (bottom)

Table 2: Statistics of Cherenkov photons from 800 MeV electrons and muons

	electron	muon
generated	138000	104000
after absorption and scattering	37500	33300
photoelectrons	610	530

Electron and muon events of 800 MeV energy

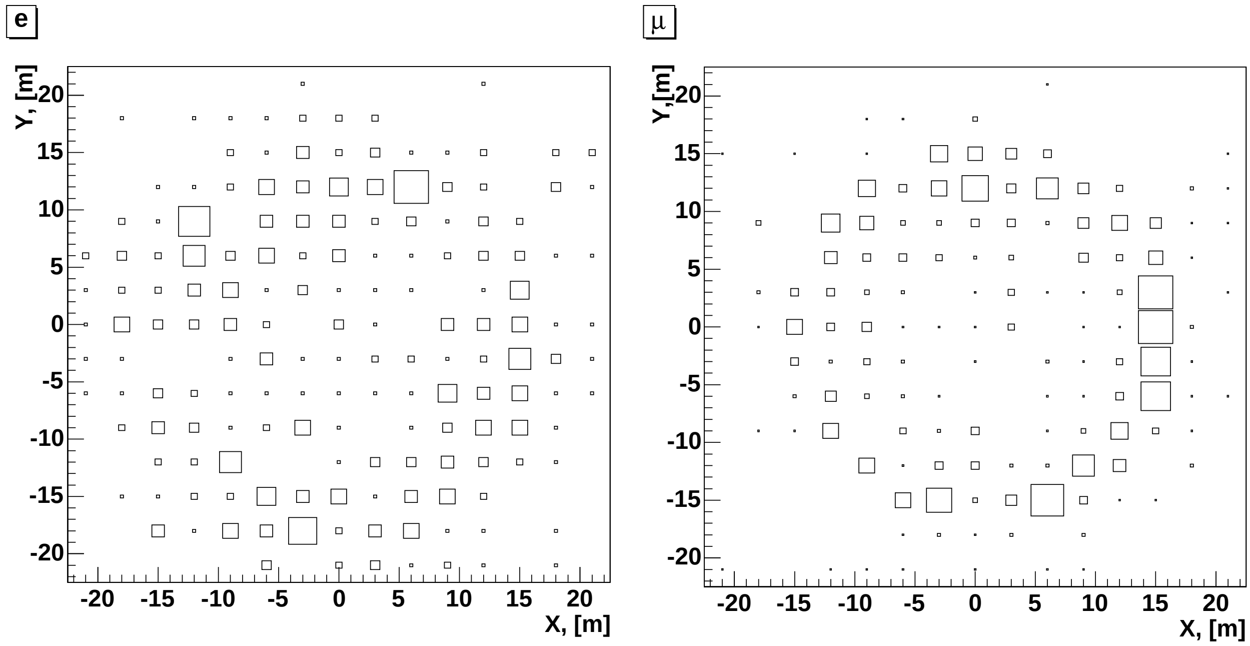

Figure 8: Cherenkov rings of a typical electron (top) and muon (bottom) event with 800 MeV total energy; the vertex is located 20 m upstream of the detector plane

Time distribution, vertex and energy reconstruction

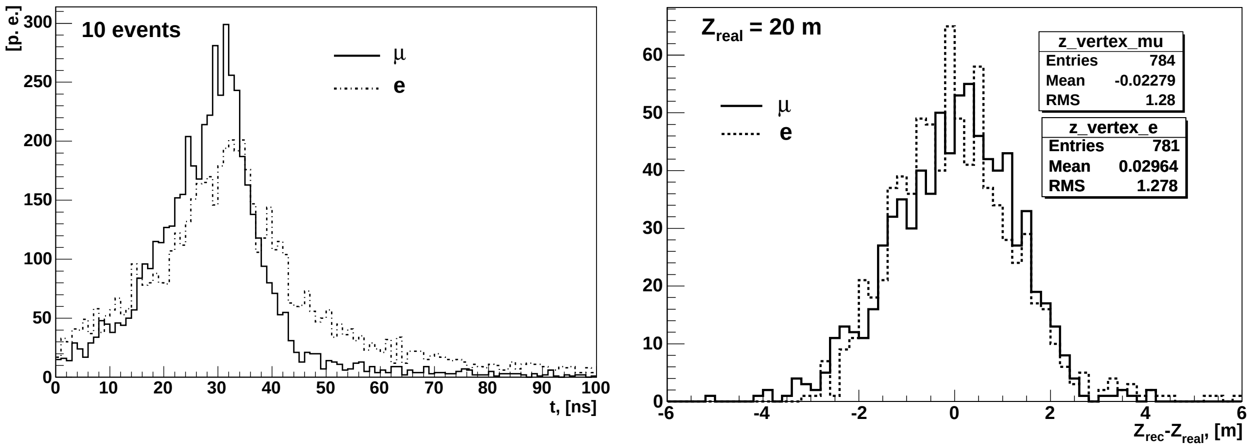

Figure 9: Time distribution of the arrival of photons from 800 MeV electrons and muons from a vertex located 20 m from the detector plane (left); reconstructed longitudinal vertex coordinate (right)

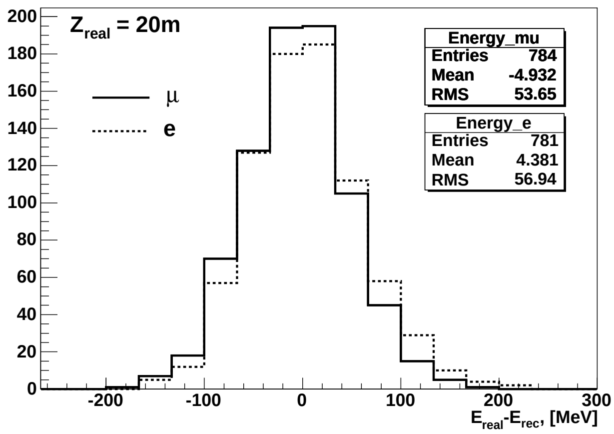

Figure 10: Energy resolution of 800 MeV electrons and muons.

Amplitude separation between electrons and muons

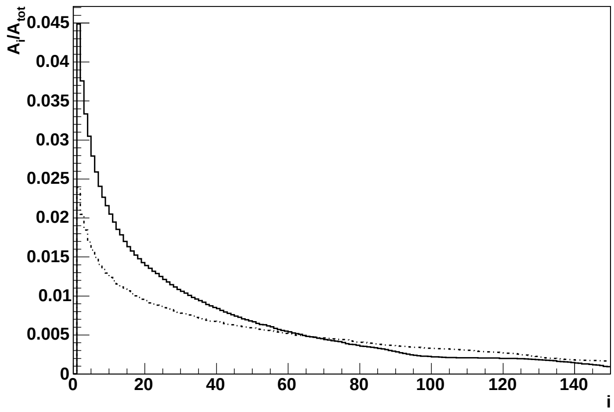

Figure 11: Average relative energy in the i.th non-zero cell when cells are ordered according to their energy content, for 800 MeV electrons (light) and muons (dark)

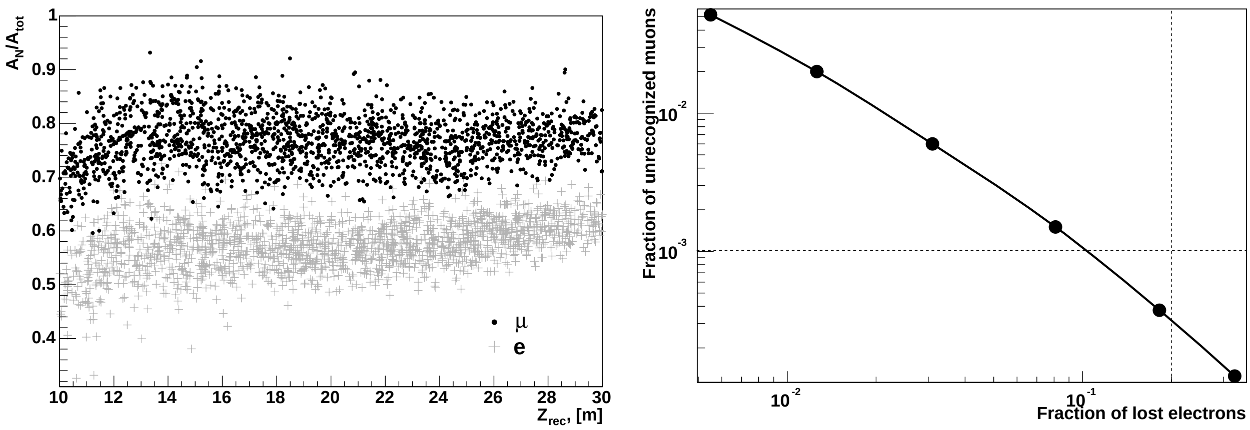

Figure 12: Separation of 800 MeV electrons and muons vs reconstructed longitudinal vertex position (left); purity versus efficiency of electrons w.r.t. muons (right); separation based on amplitude information only

Characteristics of CC quasielastic events

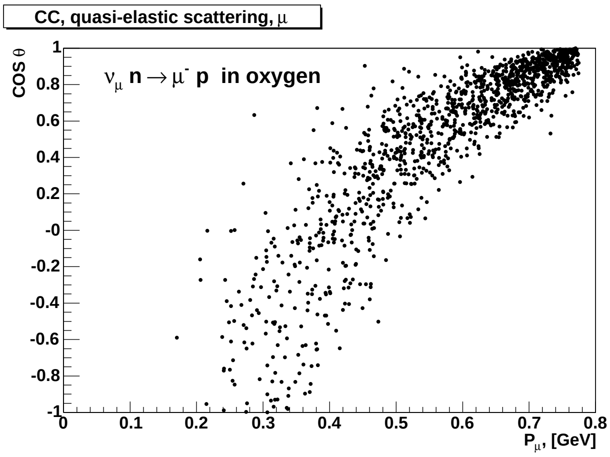

Figure 13: Cosine of the polar angle of muons from the quasielastic reaction in the ^{16}O nucleus, versus muon momentum; process generated with program NEUGEN

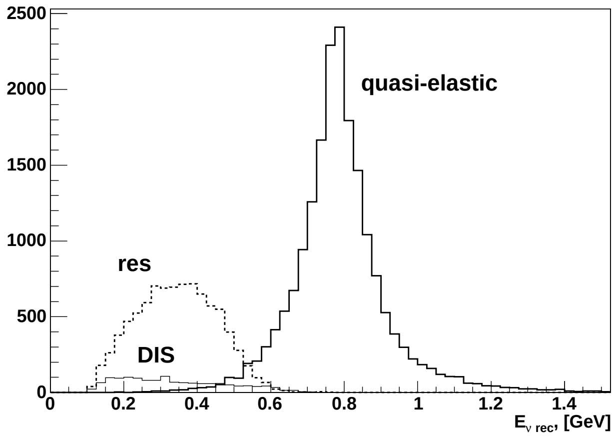

Figure 14: Neutrino energy reconstructed from events with a single muon under the hypothesis of quasieleastic neutrino-nucleon scattering.

Signal efficiencies and backgrounds

Table 3: Signal efficiencies after cuts

	CC quasielastic ν_e	CC quasielastic ν_μ
Removal of low-energy neutrinos	0.8	0.8
Removal of large-angle scattering	0.9	0.9
CC quasielastic ν_μ suppression	0.9	–
NC π^0 suppression	0.9	–
Overall	0.6	0.7

Table 4: Background percentages of unoscillated CC quasielastic ν_μ events

	CC quasielastic ν_e	CC quasielastic ν_μ
ν_e from K_{e3} and μ decays	$(0.2 \pm 0.1)\%$	–
Misidentified CC quasielastic ν_μ events	$(0.1 \pm 0.05)\%$	–
π^0 from NC production	$(0.1 \pm 0.05)\%$	–
$\pi^\pm$ from resonant NC production	–	0.1%
Sum of backgrounds	$(0.4 \pm 0.1)\%$	0.1%

Oscillation parameters $\sin^2\theta_{23}$ and Δm^2_{23}

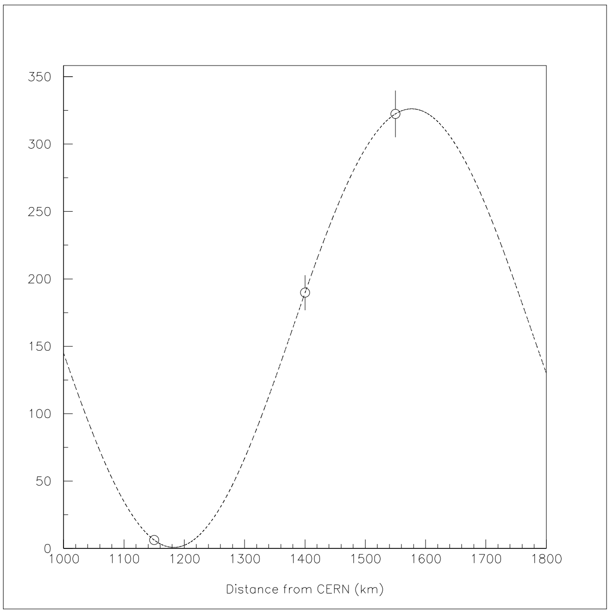

Figure 15: Fit of the CC quasielastic ν_μ rates at three different baselines in terms of $\sin^2\theta_{23}$ and Δm^2_{23}; two points correspond to one year of data taking each, the point near the minimum uses the full statistics from five years of data taking.

Table 5: Precision of $\sin 2\theta_{23}$ and Δm^2_{23}.

error on $\sin^2\theta_{23}$	$\sim 8\%$
error on Δm^2_{23}	$\sim 1\%$

Table 6: Summary of C2GT parameters and expected results from five years of running at the 2nd ν_μ oscillation maximum in search of $\nu_\mu \rightarrow \nu_\mathrm{e}$ transitions; comparison with competing projects

	C2GT	T2K	NOνA	Double-CHOOZ
Radius of instrumented detector disc [m]	150			
Height of cone of fiducial volume [m]	30			
Fiducial mass [Mt]	1.5			
No. of 400 GeV/c protons per year on target	5×10^{19}			
No. of useful π^+ decays per proton on target	0.5			
Years of running at oscillation maximum	5			
No. of ν_μ CC interactions (unoscillated)	3388			
No. of ν_μ CC quasielastic interactions (unoscillated)	2181			
CC quasielastic ν_μ selection efficiency	0.7			
No. of CC quasieleastic ν_μ events after cuts (unoscillated)	1527			
No. of background events for the ν_e signal	8.7			
Systematic error on background events	30%			
CC quasielastic ν_e selection efficiency	0.6			
Discovery potential (3σ) on $\nu_\mu \rightarrow \nu_\mathrm{e}$ probability	0.0077	0.0060		
Discovery potential (3σ) on $\sin^2\theta_{13}$	0.0039			
Discovery potential (3σ) on $\sin^2 2\theta_{13}$	0.0154			
Upper limit (90% CL) on $\boldsymbol{\nu_\mu \rightarrow \nu_\mathrm{e}}$ probability	**0.0033**			
Upper limit (90% CL) on $\sin^2\theta_{13}$	0.0016			0.0125
Same, including theoretical uncertainties		0.0015	0.0011 – 0.0021	
Upper limit (90% CL) on $\sin^2 2\theta_{13}$	0.0066			
No. of ν_e observed signal events for $\sin^2\theta_{13} = 0.05$	131			

Educated guesses of Schedule and Cost

Schedule

- 2 years for R&D, Design, Collaboration building, approval process
- 3 years for construction proper
- 1 year for installation and commissioning

Cost [MCHF]

32000 Optical Modules incl. electronics, cables	75
Mechanical Modules incl. superstructures	35
Sea operations	40
Total	150

R & D programme

1. construction and testing of an HPD; this programme has been started already with the design and fabrication, at CERN, of prototypes with a smaller diameter; the smaller than final diameter (210 mm rather than the envisaged 380 mm) is imposed by the use of existing equipment;
2. on-site measurements of sea water properties in 1000 m depth:
   - velocity of water currents
   - light absorption and scattering
   - sedimentation
   - residual background from daylight
   - bioluminescence
   - ^{40}K background.

EUROPEAN ORGANIZATION FOR NUCLEAR RESEARCH

CERN–SPSC–2004–025
SPSC–M–723
21 September, 2004

C2GT: intercepting CERN neutrinos to Gran Sasso in the Gulf of Taranto to measure θ_{13}

A.E. Ball, A. Braem, L. Camilleri, A. Catinaccio, G. Chelkov, F. Dydak, A. Elagin, P. Frandsen, A. Grant, M. Gostkin, A. Guskov, C. Joram, Z. Krumshteyn, H. Postema, M. Price, T. Rovelli, D. Schinzel, J. Séguinot, G. Valenti, R. Voss, J. Wotschack, A. Zhemchugov

Abstract

Today's most challenging issue in accelerator-based neutrino physics is to measure the mixing angle θ_{13} which is known to be much smaller than the solar θ_{12} and the atmospheric θ_{23}. Yet establishing a finite value of θ_{13} is a prerequisite for observing CP violation in the neutrino mixing matrix. A deep-sea Cherenkov experiment with 1.5 Mt mass which utilizes the modified CNGS beam in off-axis geometry, is proposed in the Gulf of Taranto. The dominant beam component consists of monochromatic muon-neutrinos of 800 MeV energy. The favourable profile of the seabed allows for a moveable experiment at three different baselines around 1200 km. The experiment will observe the oscillatory pattern of muon-neutrinos with full amplitude, will measure θ_{23} and especially Δm^2_{23} with high precision, and will be sensitive to $\sin^2\theta_{13}$ as small as 0.0016 (90% CL; theoretical uncertainties excluded).

Memorandum submitted to the Villars 2004 meeting of the SPSC

Contact person: F. Dydak (*friedrich.dydak@cern.ch*)
http://home.cern.ch/dydak/C2GT_Villars_doc.pdf